A Study of Wheat Storage Protein Monolayers by Faraday Wave Damping

D. M. Henderson,*,†,‡ K. Larsson,§ and Y. K. Rao∥

Departments of Coastal and Oceanographic Engineering and Chemical Engineering, University of Florida, Gainesville, Florida 32611, and Department of Food Technology, University of Lund, Box 124, S-221 00 Lund, Sweden

Received February 11, 1991. In Final Form: July 15, 1991

Properties of monolayers formed by wheat storage proteins (WSP) at an air/water interface were investigated by measuring the monolayers' effects on the damping of standing waves excited by vertical oscillations of a circular cylinder of water. A small concentration of a WSP monolayer increased wave-damping rates by a factor of 10, which is ~50% higher than predicted by published models. The damping rate also showed an unpredicted dependence on small changes in frequency. Cross-linking among molecules did not affect the wave-damping rates as a function of time. The WSP monolayer wet glass more effectively with increasing concentration. Damping rates were independent of whether the monolayer was spread from the solid or solution fraction.

1. Introduction

We consider here wave damping by insoluble monolayers of wheat storage proteins (WSP). Our objective is to gain insight into the properties of WSP monolayers by investigating the effects of the monolayers on the damping of large-amplitude, standing, gravity–capillary waves. To this end, we measured the amplitudes and phases of axisymmetric standing waves when the forcing that excited them was discontinued. The waves had frequencies of ~5 Hz and were subharmonically excited by the vertical oscillations of a circular cylinder of fluid. To facilitate comparisons with published theoretical predictions of damping rates, we also measured the surface shear viscosity and the surface pressure (π)–area isotherm.

Wheat storage proteins are a unique source of amphiphilic biomolecules (besides lipids) that can be spread from an organic solvent to form "insoluble" monolayers on water. Proteins in water solutions also form monolayers at the air/water interface. However, the equilibrium time for adsorption, which is mainly diffusion-controlled, is ~20 min even at concentrations of several percent (v/v). Thus, the insoluble monolayers of WSP are of particular interest. They have been investigated previously by Lundh et al.,[1] who examined the compressibility of the monomolecular film formed by WSP and related it to changes in disulfide cross-linking in the film. Herein, we examine the effects of temporal surface variations caused by waves on WSP monolayers.

The standing waves used in this investigation are known as Faraday waves; they result from the apparent change in gravity felt by the fluid in a container that is oscillated vertically. (See Miles and Henderson[2] for a review.) The particular nomral mode that is excited is the one whose natural frequency is about half that of the forcing (although the forced wave frequency is equal to half the forcing frequency). A linear stability analysis about the plane surface provides a prediction of the threshold forcing amplitude required to excite a particular mode. Benjamin and Ursell[3] did this (inviscid) analysis first; Miles[4] included viscous damping. Miles[4] also predicted the wave amplitude, given the forcing amplitude and frequency. (These theories do not include the effects of a viscoelastic monolayer at the surface.) Henderson and Miles[5] showed that the viscous predictions of the threshold forcing amplitude for waves and the wave amplitude were in good agreement with experiments on the (0,1) mode in a circular cylinder. The agreement was facilitated by the addition of a wetting agent (Kodak, Photo Flo 200) to the water, which diminished contact line effects and created a saturated film with unknown properties at the water/air interface. The (0,1) mode, which has one nodal circle and zero nodal diameters, is the one used for the investigation herein. Thus, the wavenumber was fixed for all experiments, and the frequency could vary over a small bandwidth around the natural frequency of the (0,1) mode. The experimental apparatus and procedures are described in section 3.

Theoretical estimates of wave damping due to monolayers are ubiquitous in the literature. In section 2, we posit predicted damping rates due to the lateral and bottom boundaries (e.g., Case and Parkinson)[6] and due to a viscoelastic monolayer at the surface. The latter is from Miles,[7] who generalized previous theories to include standing waves. Previous experimental investigations of damping due to monolayers have been concerned primarily with the increased damping rates of deep-water, high-frequency, small-amplitude progressive capillary waves. Oceanographic examples of wave damping have also been observed. See Davies and Vose,[8] Miles,[7] Lucassen-Reynders and Lucassen,[9] Lucassen,[10] Huhnerfuss et al.,[11-13]

† Department of Coastal and Oceanographic Engineering, University of Florida.

‡ Present address: Department of Mathematics, The Pennsylvania State University, University Park, PA 16802.

§ University of Lund.

∥ Department of Chemical Engineering, University of Florida. Present address: Hindustan Lever Limited, Research Centre, Chakala, Andheri (East), Bombay, India 400099.

(1) Lundh, G.,; Elisasson, A.-C.; Larsson, K. *J. Cereal Sci.* **1988**, *7*, 1–9.
(2) Miles, J.; Henderson, D. *Annu. Rev. Fluid Mech.* **1990**, *22*, 143–65.
(3) Benjamin, T. B.; Ursell, F. *Proc. R. Soc. London A* **1954**, *225*, 505–15.
(4) Miles, J. W. *J. Fluid Mech.* **1984**, *146*, 285–302.
(5) Henderson, D. M.; Miles, J. W. *J. Fluid Mech.* **1990**, *213*, 95–109.
(6) Case, K. M.; Parkinson, W. C. *J. Fluid Mech.* **1957**, *2*, 172–84.
(7) Miles, J. W. *Proc. R. Soc. London A* **1967**, *297*, 459–75.
(8) Davies, J. T.; Vose, R. W. *Proc. R. Soc. London A* **1965**, *260*, 218–33.
(9) Lucassen-Reynders, E. H.; Lucassen, J. *Adv. Colloid Interface Sci.* **1969**, *2*, 347–95.
(10) Lucassen, J. *J. Colloid Interface Sci.* **1982**, *85*, 52–8.

0743-7463/91/2407-2731$02.50/0

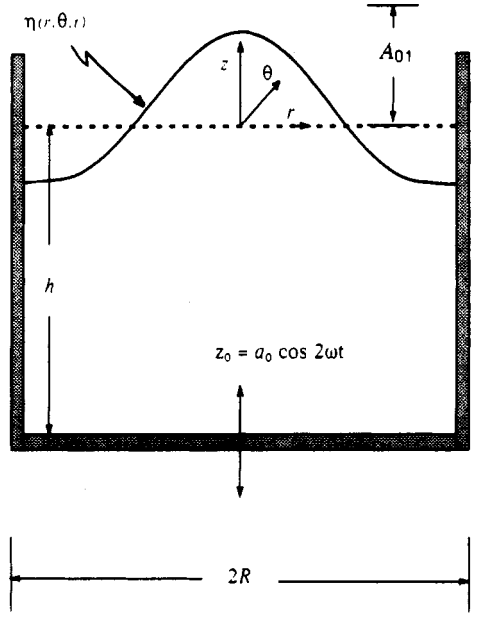

Figure 1. Definition sketch for the (0,1) mode in a circular cylinder. For all experiments $R = 3.31$ cm, $h = 3.0$ cm, $a_0 = 0.046$ cm.

and Alpers and Huhnerfuss[14] for reviews of previous theoretical, laboratory, and oceanographic field work. Experiments showed that the measured damping rates of waves on saturated films were slightly larger than predicted by an inextensible-surface model, which assumes that the surface can oscillate vertically but cannot stretch horizontally. A maximum damping rate occurred, as predicted, at some critical concentration of the film. Cini and Lombardini[15,16] investigated the excess damping of 1–50-Hz waves both theoretically and experimentally. They found a maximum damping rate at some critical frequency (and correspondingly, a critical wavenumber) for a fixed surfactant concentration. The advantages of the wave system discussed herein are that (1) measurements of the damping rates of standing waves are temporal and simpler than the spatial measurements required of progressive waves, (2) the surfactant is spread over a small surface area, (3) low-frequency, large-amplitude waves are possible, and (4) the waves are not subject to amplitude changes due to nonlinear instabilities of deep-water progressive waves. (See Perlin et al.)[17] The disadvantage of this system is that we cannot predict quantitatively the possible contribution of contact line effects to the damping rate.

2. Theoretical Considerations

In this section we provide theoretical predictions of wave-damping rates due to the bottom and lateral boundaries (see Case and Parkinson),[6] and due to a surface covered with a viscoelastic monomolecular film (see Miles[7]).

Figure 1 is a schematic of the wave basin with the water surface displacement $\eta(r,\theta,t)$ at its maximum displacement for the (0,1) mode studied herein. (The (l,m) mode has l nodal diameters and m nodal circles.) The surface displacement of the (l,m) mode is

$$\eta(r,\theta,t) = A_{lm} \cos \omega t \, J_l(k_{lm} r) \cos l\theta \tag{1}$$

where the wave amplitude, A_{lm}, depends on the forcing amplitude and frequency, as well as the cylinder's geometry, ω is the radian wave frequency (equal to half that of the forcing when the wave basin is oscillated vertically), J_l is the lth-order Bessel function, and k_{lm} is the wavenumber found from $J'_l(k_{lm}R) = 0$. When the forcing, z_0, is ceased, the wave amplitude decays at an exponential rate γ and the frequency shifts a small amount Δ, so that during wave damping, the water surface displacement can be expressed as

$$\eta(r,\theta,t) = A_{lm} e^{-\gamma t} \cos (\omega - \Delta)t J_l(k_{lm} r) \cos l\theta \tag{2}$$

The frequency shift occurs because of the difference between the natural and forced wave frequencies and is equal to

$$\Delta = (\omega^2 - \omega_{lm}^2)/2\omega \tag{3}$$

where ω_{lm} is the natural frequency of the (l,m) mode and is related to the wavenumber by the inviscid dispersion relation

$$\omega_{lm} = [(g k_{lm} + T k_{lm}^3/\rho) \tanh k_{lm} h]^{1/2} \tag{4}$$

where g is the acceleration of gravity and T and ρ are the surface tension and density of the fluid, respectively. The damping rate is

$$\gamma = \gamma_{bs} + \gamma_s \tag{5}$$

where the contribution to damping from the bottom and lateral boundaries is (e.g., Case and Parkinson[6])

$$\gamma_{bs} = \left(\frac{\mu\omega_{lm}}{2\rho}\right)^{1/2} \left[\frac{k_{lm}}{\sinh 2k_{lm}h} + \frac{1}{2R}\left(\frac{1 + (l/k_{lm}R)^2}{1 - (l/k_{lm}R)^2} - \frac{2k_{lm}h}{\sinh 2k_{lm}h}\right)\right] \tag{6}$$

Here μ is the viscosity of the fluid, R is the cylinder radius, and h is the fluid depth. The contribution to damping from the surface is γ_s. Miles[7] extended previous derivations of the damping rate due to viscoelastic monolayers at the surface to apply to standing waves to find

$$\gamma_s = C\left(\frac{\mu\omega_{lm}}{8\rho}\right)^{1/2} k_{lm} \coth k_{lm} h \tag{7}$$

where, for an insoluble monolayer

$$C = (\xi^2 + \zeta^2 + 2\zeta)/[(\xi - 1)^2 + (1 + \zeta)^2] \tag{8}$$

He represented the dimensionless surface elasticity and viscosity as

$$\xi = (\mu\rho\omega_{lm}^3/2)^{-1/2} k_{lm}^2 \Gamma_0 (d\pi/d\Gamma_0) \tag{9}$$

and

$$\zeta = (\mu\rho\omega_{lm}/2)^{-1/2} k_{lm}^2 (\eta_1 + \eta_2) \tag{10}$$

where Γ_0 is the surface concentration of surfactant, η_1 is the dilatational viscosity, and η_2 is the shear viscosity of the film. The surface pressure, π, is the difference between the surface tensions of a clean surface (72.4 dyn/cm) and one with a monolayer. When the film is inextensible, $\xi \to \infty$ and $C = 1$. When the surface is clean, $C = 0$, and the contribution to damping from the surface, which is of lower

(11) Huhnerfuss, H.; Lange, P.; Walter, W. *J. Mar. Res.* **1984**, *42*, 737–59.
(12) Huhnerfuss, H.; Lange, P.; Walter, W. *J. Colloid Interface Sci.* **1985**, *108*, 430–41.
(13) Huhnerfuss, H.; Lange, P.; Walter, W. *J. Colloid Interface Sci.* **1985**, *108*, 442–50.
(14) Alpers, W.; Huhnerfuss, H. *J. Geophys. Res.* **1989**, *94*, 6251–265.
(15) Cini, R.; Lombardini, P. P. *J. Colloid Interface Sci.* **1978**, *65*, 387–89.
(16) Cini, R.; Lombardini, P. P. *J. Colloid Interface Sci.* **1981**, *81*, 125–31.
(17) Perlin, M.; Henderson, D.; Hammack, J. *J. Fluid Mech.* **1990**, *219*, 51–80.

order than eq 7, is

$$\gamma_s^{(c)} = 2(\mu/\rho)k_{lm}^2 \quad (11)$$

3. Experimental Procedures

3.1. Materials. The cereal endosperms used in these experiments contain storage proteins assembled in spherical aggregates, which are known as protein bodies. These proteins are almost insoluble in water and thus can be spread on the air/water interface after they are dissolved in an ethanol/water solvent mixture. Bungenberg de Jong and Klaar[18] analyzed the separation and colloidal behavior of WSP. The two main fractions are gliadins, which are soluble in aqueous ethanol, and glutenins, which are the insoluble residue. The gliadins are mainly a low molecular weight fraction (<80 000 Da) whereas, glutenins have higher molecular weights (cf. Lundh et al.[1]).

Gluten from Amylum, (Alst) was lipid-depleted by washing in *n*-butanol and separated according to the Osborne fractionation into a gliadin fraction, soluble in 70% (v/v) ethanol/water solution, with glutenin as the insoluble residue. The protein solution was spread directly on the water surface using an Agla microsyringe (Burroughs-Wellcome). The concentration of the solution was ~3 mg/mL. In one experiment, the glutenin powder was used directly on the water surface for monolayer formation.

3.2. Surface Pressure (π)–Area Measurements. The surface pressure–concentration isotherm was measured using a Langmuir film balance. (The concentration was not converted to area because the molecular weight of WSP is not known accurately.) The surface pressure was measured with a Wilhelmy plate connected to a Statham transducer readout. The monolayer tray was made from Plexiglass. The trough was cleaned using distilled water, the last traces of which were removed by suction. (We note that the wave experiments were conducted in glass cylinders; see section 3.4.) Doubly distilled water, which was filtered through 11-μm Whatman paper, was used as the subsolution and was poured about 2–3 mm above the rim of the trough. The surface of the subsolution was cleaned by moving a wax-coated glass slide across the trough and then sucking the impurities with a capillary connected to a vacuum pump. Cleanliness was checked by ensuring that measurements of surface tension during complete compression of the barriers corresponded with that of pure water. Measurements were accurate to 0.5 dyn/cm. About 1 mg/m^2 of substance was spread evenly on the water surface using the Agla microsyringe. After 5 min, during which the solvents were allowed to dissolve in the water phase, the monolayers were compressed slowly. The data obtained from these measurements are presented in Figure 3b along with the measurements of surface pressure obtained in the wave basin before each wave-damping experiment.

3.3. Surface Shear Viscosity Measurements. The surface shear viscosity of WSP monolayers was measured using an indigenously built, deep-channel surface viscometer. A detailed description of such a device is in, for example, Wei and Slatterly.[19] The viscometer consisted of two concentric aluminum cylinders that created an annulus of width $y_0 = 0.87$ cm. The annulus had inner and outer circumferences of $2\pi 4.80$ and $2\pi 5.67$ cm, respectively. The annulus was filled with doubly distilled water to a depth of $d = 0.655$ cm. The surface was cleaned, and a known volume of surfactant was spread as described in section 3.2. A Teflon particle was floated on the surface at the annulus' centerline. The floor of the annulus was then steadily rotated at a speed of $V_f = 3.0$ cm/s, while the annulus remained stationary. The speed of the particle, V_p was measured, and the surface shear viscosity was calculated from

$$\eta_2 = (\mu y_0/\pi)[8V_f/\pi V_p e^{\pi d/y_0} - 1] \quad (12)$$

where all variables are in CGS units and we have assumed that the viscosity of air is negligible compared to that of water. A derivation of this equation can be found in Wasan, Gupta, and Vora.[20] The variation of viscosity with concentration is shown in Figure 3c.

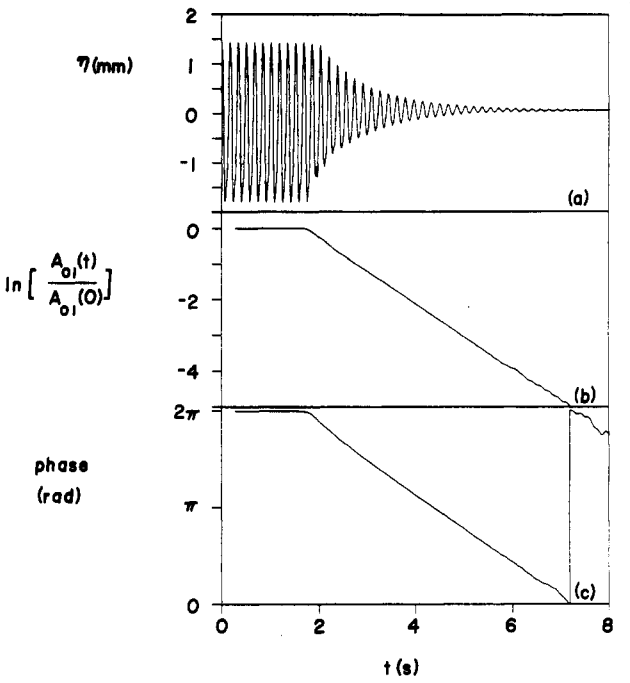

Figure 2. (a) Time series, (b) natural log of the amplitude normalized by the steady-state amplitude, and (c) phase of a 5.90-Hz wave when the concentration of the WSP monolayer was 6.10 mg/m^2.

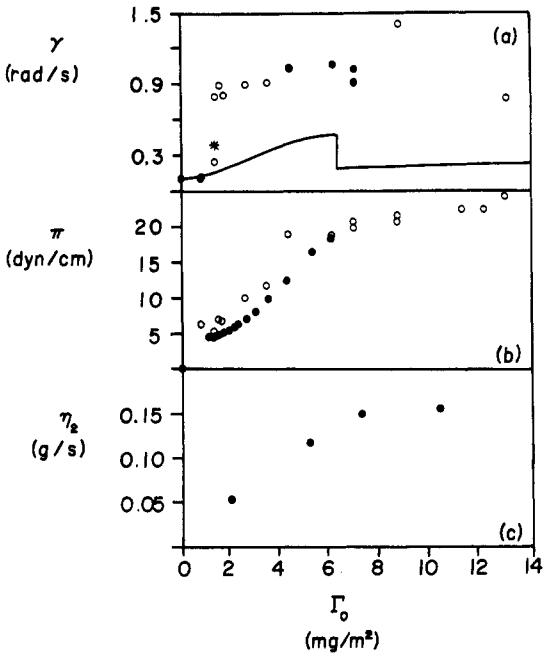

Figure 3. (a) Damping rates of 5.95- (●) and 6.00- (○) Hz waves where * corresponds to the one experiment in which WSP was applied to the water surface in solid form. The solid curve represents calculations from eqns 5–10. (b) Surface pressure obtained from wave data (○) and from the Langmuir tray (●). (c) Surface shear viscosity, as a function of WSP concentration.

3.4. Wave Excitation and Damping. The apparatus for wave experiments comprised glass circular cylinders, a computer system, an electromagnetic shaker with feedback, and an in situ wave gauge. The cylinders were crystallizing dishes made of Pyrex glass with radii of $R = 3.31 \pm 0.01$ cm. They were cleaned by rinses in chromic acid, tap water, distilled water, and acetone and then heated at 80 °C. (The acetone was from Fisher Scientific

(18) Bungenberg de Jong, H. L.; Klaar, W. *Trans. Faraday Soc.* **1932**, *28*, 27–68.

(19) Wei, L.; Slattery, J. C. *Colloid and Interface Science*; Kerker, M., Ed.; Academic Press Inc.: New York, 1976; pp 399–420.

(20) Wasan, D. T.; Gupta, L.; Vora, M. K. *AIChE J.* **1971**, *17*, 1287.

and was 99.5% pure.) A different cylinder was used for each experiment. Doubly distilled water was added to a cylinder and the surface vacuumed with a pipet until the depth was $h = 3.00 \pm 0.02$ cm. A given amount of WSP was applied to the surface with the Agla syringe, and the surface tension was measured with a Wilhelmy plate as described in section 3.2.

An electrodynamic shaker, Bruel & Kjaer minishaker Type 4810, oscillated the cylinder vertically. A noncontacting proximity sensor (Kaman Model KD-2310) monitored the shaker motion and provided a signal to a servocontroller. The controller acted as a feedback device to ensure that the actual motion followed the programmed one; additionally, it provided measurements of the forcing amplitude, accurate to 0.005 mm. For all experiments, the forcing amplitude was 0.046 cm. The command signal to the shaker was provided by a MicroVAX Workstation II, which had analog input and output systems with two separate, programmable real-time clocks.

Vertical oscillations of the cylinder excited Faraday waves with a frequency half that of the forcing. An in situ, glass, capacitance-type gauge measured a time series of the surface displacement. The gauge diameter was 1.15 mm (the wavelength was ~54 mm). The gauge signal was low-pass-filtered at 30 Hz twice by a Krohn-Hite Model 3323 analog filter, which also produced a 20-dB gain. It was then digitized at 350 Hz by the computer. The gauge was calibrated by comparing its signal to mechanical measurements of surface displacement with a Lory Type C point gauge combined with a dial micrometer accurate to 0.01 mm. The wave amplitudes were measured with an accuracy of 0.01 mm.

To determine damping rates, first we measured the time series of the water surface displacement before and after the shaker was turned off. Second, we complex-demodulated the time series at half the forcing frequency to obtain the amplitude and phase of the surface displacement averaged over 100 points (or 0.35 s). Figure 2 shows a time series and the complex-demodulated amplitudes and phases for a typical experiment. The amplitudes in Figure 2b are shown on a natural log scale; thus the slope of the curve is the damping rate, which is accurate to ±0.01 rad/s. The phase of the wave, shown in Figure 2c, is a measure of the actual wave frequency, accurate to 10^{-6} Hz. The horizontal line from about 0 to 2 s indicates that while forced, the wave had a frequency equal to half that of the forcing. After the forcing was discontinued, the wave frequency changed by an amount Δ, which is related to the difference between the natural and forced frequencies. Thus, the natural frequencies of the waves were computed from eq 3 and measurements of Δ.

4. Results and Discussion

4.1. Wave Damping as a Function of Concentration. Figure 3 shows measurements and predictions of damping rates, and measurements of surface pressure and surface shear viscosity as functions of the WSP concentration, Γ_0. The surface pressure measurements that were obtained from the Langmuir balance (see section 3.2) show a smooth π–Γ_0 isotherm, with saturation occurring at $\Gamma_0 \approx 6.1$ mg/m^2. The surface pressure measurements that were obtained from the wave basin show scatter, which probably resulted from the loss of WSP to the basin walls. When $\Gamma_0 > 6.1$ mg/m^2, no additional WSP seemed to spread, as indicated by the pressure–area isotherm. The shear viscosity, measured as described in section 3.3, was maximum at the saturation concentration of ~6.1 mg/m^2 and changed little with further amounts of WSP. The thickness of a uniform monolayer at $\Gamma_0 = 6$ mg/m^2 was ~42 Å (using a specific volume of 0.72 μL/g).

The theoretical estimate of damping rate shown in Figure 3a was calculated from eqs 5–10 as follows. We used the actual wave frequency in eqs 6 and 7 instead of the natural frequency. In eq 10, we used a dilatational viscosity, η_1, of zero, since we have no knowledge of its value. The shear viscosity, η_2, was determined from a linear extrapolation of the data shown in Figure 3c. We tried many different methods to estimate the slope of the π–Γ_0 curve, and therefore, the surface elasticity (eq 9), including

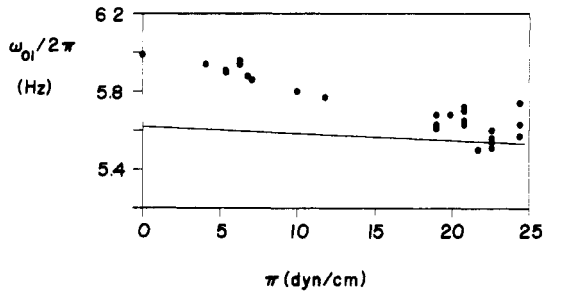

Figure 4. Measurements (●) and predictions (—) of the natural frequency of the (0,1) mode.

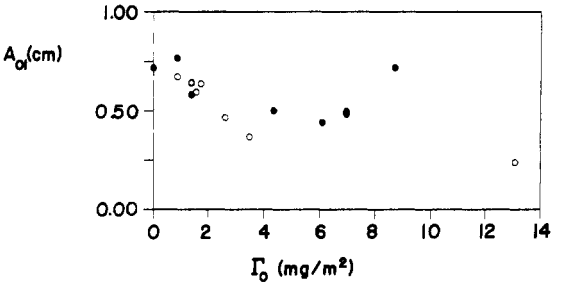

Figure 5. Measurements of the steady-state wave amplitudes as a function of WSP concentration for 5.95- (●) and 6.00- (○) Hz waves.

a least-squares quadratic fit and a power law fit. Although the shape of the γ–Γ_0 curve depends crucially on the choice of $\pi(\Gamma_0)$, the maximum value of γ does not. Thus, in Figure 3a we show an order of magnitude, theoretical estimate of the damping rates by representing $\pi(\Gamma_0)$, such that

$$d\pi/d\Gamma_0 = 3.2 \qquad 0 < \Gamma_0 < 6.2 \tag{13a}$$

$$d\pi/d\Gamma_0 = 0.4 \qquad \Gamma_0 > 6.2 \tag{13b}$$

When $\Gamma_0 < 1.5$ mg/m^2, the waves damped at ~0.1 rad/s, as they did when the surface was clean ($\Gamma_0 = 0$). This damping rate corresponded to an observed decay time of ~50 s. The damping rate increased dramatically, by a factor of ~10, at $\Gamma_0 \approx 1.5$ mg/m^2 when the surface pressure was ~5 dyn/cm. A damping rate of 1 rad/s corresponded to an observed decay time of ~5 s as is apparent in the time series of Figure 2a. The theory underestimated the observed increase in damping rate by ~50%, regardless of the representation of the $\pi(\Gamma_0)$ curve. For $\Gamma_0 > 6.1$ mg/m^2, the observed damping rate attained a maximum value and then decreased with additional WSP. The theory cannot predict this variation, because the corresponding changes in surface pressure and surface shear viscosity are almost negligible. We note that in the limit of an inextensible surface ($C = 1$) the damping rate predicted by eq 7 is $\gamma = 0.31$ rad/s.

There are three known factors that are not included in the theory. The first is the contribution to damping due to the contact line. For a clean surface, the wave decayed ~10% faster than predicted by eq 5 using eq 11; thus, we can estimate that the contact line was responsible for ~10% of the damping rates shown in Figure 3a. We assume that contact line dynamics are responsible for the scatter in the data of Figure 3a (as well as that in Figures 4 and 5), because the effects of the contact line are different each time a cylinder is used. However, it is likely that the contact line became less important with increasing concentration. Figure 4 shows observations and predictions from eq 4 of natural frequencies of the waves. Measurements of the natural frequency (see section 3.4) showed that the largest discrepancy was in the absence of a mono-

layer. Henderson and Miles[5] showed that measurements of the natural frequency of the (0,1) mode were well-predicted by eq 4, when a wetting agent was added to the water. Since the disagreement between predictions and measurements occurs with the lack of the wetting agent, we conclude that the contact line is responsible. Figure 4 shows that when the surface pressure, and correspondingly the WSP concentration, increases, the disagreement between theory and observations decreases. Thus, the importance of the contact line decreases with increasing concentration, so that it is unlikely that the variation in damping rate observed for $\Gamma_0 > 6.1$ mg/m^2 is due to contact line effects. The data of Figure 4 also show that the WSP monolayer wetted glass more effectively with increasing WSP concentration. We note that damping rates do affect the dispersion relation (eq 4) with γ_{bs} decreasing the natural frequency a few percent and γ_s either increasing or decreasing the natural frequency a few percent. However, this small effect is negligible in the comparison of data and theory in Figure 4.

The second factor ignored in the theory is the surface dilatational viscosity, η_1, which we set to zero. If damping rate varies with η_1 with the dependence assumed in eq 10, then η_1 could not have caused the large difference in observed and predicted damping rates. As η_1, η_2, or $d\pi/d\Gamma_0$ becomes large, the damping rate approaches a maximum comparable to that shown by the solid curve in Figure 3a. Thus, either the surface dilatational viscosity is not responsible for the large discrepancy between predicted and observed damping rates, or the predicted dependence of γ on η_1 in eq 10 is inadequate. Regardless, we cannot use the experiments herein to estimate a value for η_1. For $\Gamma_0 > 6.1$ mg/m^2, it is likely that the dilatational viscosity is about constant, as are the shear viscosity and surface pressure; hence the observed variations in damping rate for $\Gamma_0 > 6.1$ mg/m^2 are probably not in consequence of η_1.

The third factor neglected in the theory is cross-linking among molecules. It is known that the gliadin fraction of WSP in native form contains intramolecular disulfide bridges only, but as the peptide chain unfolds at the air/water interface, it seems quite possible that intramolecular disulfide bridges also may form at the interface. Cross-linking can cause flows within the monolayer that are not considered in the boundary condition that leads to eq 7. These flows could cause gradients in surface pressure that would increase the damping rate as do gradients due to the film's compressibility. Thus, cross-linking among molecules cannot be overruled as a possible explanation for the observed damping rates. Lundh et al.[1] showed that the degree of cross-linking increased with compression. Thus, the variation in damping rate observed for $\Gamma_0 > 6.1$ mg/m^2 may also be the result of cross-linking.

Lundh et al.[1] showed that cross-linking changed the size of the WSP molecules as a function of time. To determine if this time dependence also affected the damping rates, we measured the damping rates for fixed concentrations at 5-min intervals. For one experiment, we monitored the damping rate for 1 h. In all cases, the damping rate did not change significantly with time.

The monolayer behavior of WSP spread from the solid phase (the glutenin fraction) also exhibits cross-linking by disulfide bridges at the air/water interface (see Lundh et al.[1]). In the experiment represented by * in Figure 3a, ~0.5 mg of glutenin from the solid phase was spread as particles on the water surface. After 20 min, the surface pressure was 5.4 dyn/cm. The effect on wave damping

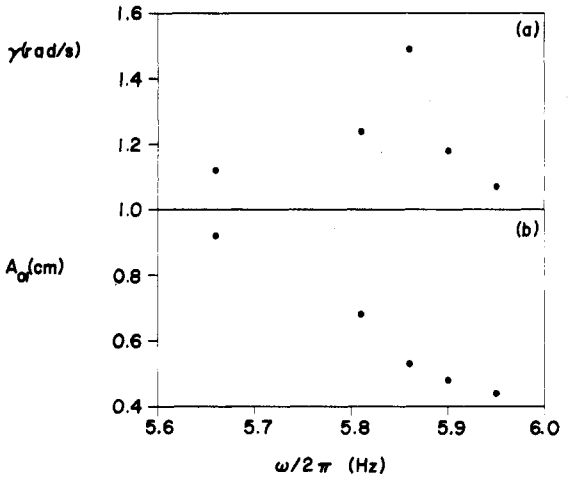

Figure 6. Measurements of the (a) damping rates and the (b) steady-state wave amplitudes as a function of wave frequency: $\Gamma_0 = 6.10$ mg/m^2, $\pi = 10$ dyn/cm.

was consistent with that of the film from the WSP solution (the gliadin fraction) with the corresponding surface pressure.

Figure 5 shows the observed steady-state amplitudes of the Faraday waves, whose damping rates are displayed in Figure 3a, as a function of WSP concentration. These data show that the wave amplitudes were fairly large, causing wave slopes on the order of $A_{01}k = 0.5$, and that the monolayers were undergoing a significant amount of straining. Theories (e.g., Miles[4]) that incorporate the change in surface tension caused by the monolayer (but not the rheological properties of the monolayer) predict that wave amplitudes decrease very slowly with increasing concentration. Although there is much scatter in the data, the wave amplitudes do tend to decrease (more rapidly than predicted by theory) with increasing concentration. The large observed variation, as well as the scatter, in wave amplitude could be the result of contact line dynamics. The natural frequencies of the waves also decreased much more rapidly with increasing concentration than predicted (see Figure 4), and amplitudes depend on the natural frequency. We cannot rule out the possibility that the rheological properties of the WSP monolayer also played a role. More control over contact line dynamics is necessary to investigate this possibility.

4.2. Wave Damping as a Function of Frequency. Figure 6 shows the damping rates and steady-state amplitudes measured for waves with different frequencies on the same monolayer. The observed dependence of damping rate on frequency is not predicted by eqs 6 and 7. Cini and Lombardini[16] saw a frequency dependence in their progressive-wave experiments that they explained analytically.[15] The wavenumber of progressive waves changes with frequency as predicted by eq 4, and there is a maximum damping rate associated with some critical wavenumber. Conversely, the wavenumber of standing waves is fixed by the basin geometry, so a frequency dependence in the damping rates of a single mode arises only by using the forced, instead of natural, wave frequency in eqs 6 and 7. However, this frequency variation is quite small for the frequency range examined herein and is monotonic. The observed frequency dependence in damping rate indicates that some property of the WSP monolayer is frequency-dependent. A likely candidate is the dilatational viscosity, which measures the surface's resistance to area changes, which depend on the wave amplitude. Figure 6b shows the amplitudes of the waves whose damping rates are shown in Figure 6a. We find no

obvious correspondence between the damping rates and wave amplitudes. It is also possible that the effect of cross-linking on wave damping is frequency-dependent. We note that since the cylinder, water, and monolayer were the same for all the data in Figure 6, contact line dynamics were also the same and did not cause the observed variations in damping rate.

5. Conclusions

We make the following conclusions from this investigation of the effects of insoluble monolayers of wheat storage protein on the damping rates of large-amplitude, gravity–capillary standing waves:

1. The presence of a small concentration of a WSP monolayer increased wave damping rates by a factor of 10.

2. The observed damping rates were 50% larger than predicted by a (standard) theory that includes the monolayer's elasticity and surface shear viscosity. The surface dilatational viscosity of WSP monolayers was not responsible for this large discrepancy. Cross-linking among molecules cannot be ruled out as a possible explanation.

3. Cross-linking among molecules did not affect the wave damping rates as a function of time.

4. The WSP monolayer wet glass more effectively with increasing concentration.

5. WSP monolayers spread from the solid phase (the glutenin fraction) affected wave damping the same as WSP monolayers spread from the ethanol solution (the gliadin fraction).

6. The effect of the WSP monolayer on wave-damping rates depended on small changes in the frequency of surface straining.

Acknowledgment. These experiments are part of an ongoing research program in collaboration with Professors D. Shah and J. Hammack at UF. Financial support for the experimental facilities was provided by the Office of Naval Research through Contract N00014-89-J-1335.